Materials Science and Engineering B 178 (2013) 94–98

Contents lists available at SciVerse ScienceDirect

Materials Science and Engineering B

journal homepage: www.elsevier.com/locate/mseb

Short communication

Development of a very fast spectral response measurement system for analysis of hydrogenated amorphous silicon solar cells and modules

J.A. Rodríguez[a,*], M. Fortes[b], C. Alberte[a], M. Vetter[a], J. Andreu[a]

[a] Dept. Technology, Development & Innovation, T-Solar Global S.A., Parque Tecnológico de Galicia, Avda. de Vigo 5, E-32900 San Cibrao das Viñas (Ourense), Spain
[b] Departamento de Electrónica e Computación, Universidade de Santiago de Compostela, 15782 Santiago de Compostela, Spain

ARTICLE INFO

Article history:
Received 8 June 2012
Received in revised form
10 September 2012
Accepted 11 October 2012
Available online 29 October 2012

Keywords:
Solar cell
Amorphous silicon
Spectral response
LED

ABSTRACT

An important requirement for a very fast spectral response measurement system is the simultaneous illumination of the solar cell at multiple well defined wavelengths. Nowadays this can be done by means of light emitting diodes (LEDs) available for a multitude of wavelengths. For the purpose to measure the spectral response (SR) of amorphous silicon solar cells a detailed characterization of LEDs emitting in the wavelength range from 300 nm to 800 nm was performed. In the here developed equipment the LED illumination is modulated in the frequency range from 100 Hz to 200 Hz and the current generated by each LED is analyzed by a Fast Fourier Transform (FFT) to determine the current component corresponding to each wavelength. The equipment provides a signal to noise ratio of 2–4 orders of magnitude for individual wavelengths resulting in a precise measurement of the SR over the whole wavelength range. The difference of the short circuit current determined from the SR is less than 1% in comparison to a conventional system with monochromator.

1. Introduction

T-Solar Global (T-Solar) is manufacturer of very large 2.6 m × 2.2 m amorphous silicon (a-Si:H) single junction thin film modules using Applied Materials SUNFAB technology. The actual design of the very large modules consists of various parallel strings of 216 solar cells with a width of 1 cm connected in series. The homogenous deposition of all the different layers implemented in the p–i–n structure of the solar cell is a challenge and e.g. high uniformity of film thickness is necessary to assure high module efficiency. Since a large number of solar cells are connected in series, a very uniform current generation is desired along the module. The locally generated current, i.e. the short circuit current density (J_{sc}) in the solar cell can be calculated from the spectral response (SR) measurement of a small illuminated area, however this kind of SR measurements usually are performed on laboratory scale using a monochromator as the light source and a lock-in amplifier technology, which is a time consuming method (about e.g. 15 min per SR in the wavelength range from 300 nm to 800 nm in our lab) and therefore is not suitable for the creation of mappings of J_{sc} values with a resolution of a few cm of a very large area module as fabricated in T-Solar.

We are developing a very fast spectral response (VFSR) measurement system [1,2] with the objective to measure the SR in about 1 s using simultaneous light generation of high power light emitting diodes (LEDs) operating at different frequencies. Applying a Fast Fourier Transform (FFT) analysis to the generated solar cell current allows to extract the SR in a small illuminated area (approx. 0.5 cm diameter).

Several other research groups have investigated this kind of rapid measurement technique, mainly focusing on light coupling by fibre optics and applying lock-in amplifying technology for the signal (solar cell current) detection [1–5]. Specially in earlier work, LEDs with very high light intensity were not available for the whole wavelength range between ultraviolet (UV) and near infrared (NIR) (300–1100 nm), so lock-in technology still needed to be applied to detect the small solar cell currents resulting in complex programming work to achieve fast reliable measurements. In addition the application of optical fibres further results in poor utilization of the LED light and consequently measurements systems are not very compact and expensive. Since a few years, high intensive compact and cheap LEDs are available for the whole UV/Visible (VIS)/NIR wavelength range in the commercial market making possible the implementation of another type of light coupling technique not making necessary lock-in amplifiers, resulting in a very compact and low cost measurement equipment. Our objective is to combine the very compact SR measurement equipment with an *XY* displacement system to generate spatial SR mappings with a resolution in the range of centimetres making possible to locate low current generation areas in modules. Then, deposition process optimization can be performed to increase the overall module current. The main focus is to develop rapidly a system for the measurement

* Corresponding author. Tel.: +34 988 540 254; fax: +34 901021034.
E-mail address: jose.rodriguez@tsolar.eu (J.A. Rodríguez).

0921-5107/$ – see front matter © 2012 Elsevier B.V. All rights reserved.
http://dx.doi.org/10.1016/j.mseb.2012.10.009

Table 1
Comparison of the technical data sheet values with the experimental data obtained at our lab for the 16 selected LEDs.

LED code	Data sheet peak wavelength (nm)	Experimental peak wavelength (nm)	FWHM (exp.) (nm)	Data sheet DC bias		Experimental DC bias		Experimental AC amplitude		Structure
				V (V)	I (mA)	V (V)	I (mA)	(V)	(mA)	
L1	370	376	11	3.90	10.0	3.50	30.5	0.3	23	AlGaN
L2	385	383	11	3.50	20.0	3.55	47.0	0.3	35	InGaN
L3	400	395	12	3.70	20.0	3.50	18.5	0.4	26	InGaN
L4	415	412	14	3.70	30.0	3.35	24.0	0.3	21	InGaN
L5	470	470	31	3.20	30.0	3.40	18.0	0.4	20	InGaN
L6	510	501	23	3.40	20.0	3.25	18.0	0.5	25	InGaN
L7	525	524	38	3.20	20.0	3.00	37.0	0.3	33	InGaN
L8	565	562	23	2.00	20.0	3.50	18.0	0.5	34	GaP
L9	596	593	15	2.10	20.0	2.00	14.0	0.3	25	AlGaInP
L10	625	641	16	2.20	20.0	2.45	35.0	0.5	41	AlGaInP
L11	670	672	25	1.80	20.0	1.80	22.0	0.2	31	GaAlAs/GaAlAs
L12	680	683	21	1.90	20.0	2.20	47.0	0.3	33	GaAlAs
L13	720	721	24	2.00	50.0	1.80	34.0	0.2	37	AlGaAs/AlGaAs
L14	760	755	25	1.20	20.0	1.65	26.0	0.3	57	AlGaAs/AlGaAs
L15	780	772	27	1.70	50.0	2.00	43.0	0.3	33	AlGaAs/AlGaAs
L16	800	795	30	1.80	50.0	1.65	66.0	0.3	67	AlGaAs

of large area single junction a-Si:H solar cells which are actually implemented in T-Solar modules. Another application is to use the VFSR equipment to perform in-line diagnostics to identify possible process errors once the solar cell fabrication is completed (after P3 laser scribe process) and the module is still not laminated, e.g. contacting the solar cells at the panel back side with point probes.

2. Theory

2.1. Photosensitivity and quantum efficiency

The SR of a solar cell is the photosensitivity (R) measured along the spectrum of light. The R (expressed in A/W) represents the intensity of the photovoltaic effect depending on the incoming light for a given wavelength, it allows to determine how much current is generated by a solar cell for a specific irradiation and for each wavelength in the entire spectrum. The SR is also associated to the external quantum efficiency (EQE, expressed in %) which represents the number of electron/hole pairs generated in the cell by the incident photon flux [6]. Both parameters are linked by the following equation:

$$\mathrm{EQE} = \frac{Rhc}{q\lambda} \tag{1}$$

where: q is the electron charge of one electron ($q = 1.602 \times 10^{-19}$ C), h is the Plank's constant ($h = 6.626 \times 10^{-34}$ J s), c is the speed of light ($c = 3 \times 10^{17}$ nm/s), λ is the wavelength of the incident light (nm).

The SR is usually used to extract information about recombination at front and rear contacts, diffusion or drift lengths of carriers, width of the depletion region and light trapping properties among the most important [7,8].

2.2. Differential spectral response method

Traditionally, the differential spectral response method (DSR method) is based on detection by an lock-in amplifier of the solar cell response (solar cell current) to a modulated (AC) monochromatic test light under simultaneous exposure of a white bias (DC) light of irradiance in the range of 1 sun illumination. In another variation an incandescence lamp filtered with a monochromator or a set of spectral filters is used as a monochromatic test light source, while a solar simulator is used as a bias light source [9]. Moreover, in the case of non-linear devices it is necessary to use a chopped monochromatic beam [10].

Here is presented a novel DSR experimental set-up using LED illumination which changes the light source but not the basic procedure of the method.

The principle of the DSR method [10] is to compare the current of a reference photodiode and the current of the solar cell under test illuminated simultaneously by the same light source under STC (standard test conditions) [11]. Monitoring simultaneously these two currents for each wavelength and knowing the calibration factor ($F(\lambda)$) for the reference cell we can calculate the R of the solar cell under test and, thus, the EQE and the short circuit current I_{sc} (see below).

2.3. Determination of the calibration factor, spectral response and J_{sc}

Previously of measuring the solar cell in the VFSR equipment, its reference photodiode current is compared to that of a calibrated photodiode located in the place of the solar cell. In this way we determine the $F(\lambda)$. Then, the solar cell under test is illuminated simultaneously with the reference photodiode.

$$R_{\mathrm{cell}}(\lambda) = \frac{I_{\mathrm{cell}}(\lambda)}{I_{\mathrm{ref}}(\lambda)} \cdot F(\lambda) \cdot R_{\mathrm{c}}(\lambda), \quad \text{where } F(\lambda) = \frac{I_{\mathrm{ref}}(\lambda)}{I_{\mathrm{c}}(\lambda)} \tag{2}$$

I_{cell} is the current generated in the solar cell under test, I_{ref} the current in the reference photodiode and I_{c} the current in the calibrated photodiode.

To calculate the I_{sc} of the solar cell we integrate the product of the measured $R(\lambda)$, the irradiance ($G(\lambda)$) of the AM1.5 spectrum and the surface of the solar cell under test as shown in the following equation (with integration interval from λ_i to λ_f):

$$I_{\mathrm{sc}} = \int G(\lambda) \cdot R(\lambda) \cdot S \, d\lambda;$$

$$\text{where } [G] = \mathrm{W/m^2}, [S] = \mathrm{m^2}, [I_{\mathrm{sc}}] = \mathrm{A} \tag{3}$$

3. Experimental

To build up the VFSR measurement system we use coloured LEDs of different wavelengths as light source. A coloured LED is not monochromatic, but has a spectral bandwidth of tens of nanometres in the visible range. However, the use of LEDs provides several important advantages compared to the conventional monochromator-based lightsource: First of all, LEDs can be used without optical components for spectral filtering, resulting in

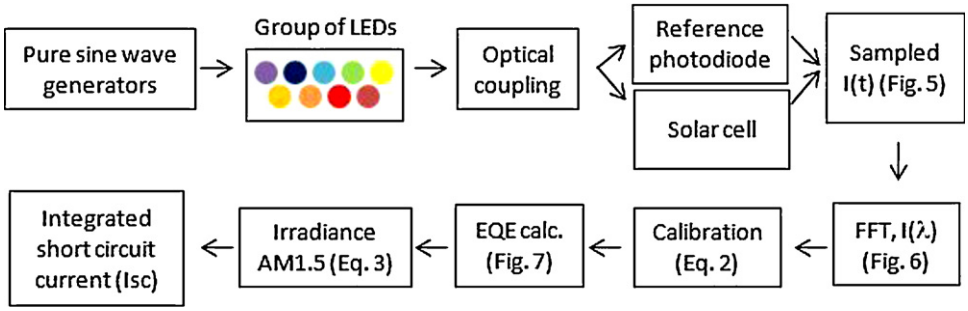

Fig. 1. Diagram of the VFSR measurement system.

already high uniformity irradiance on the test solar cell when adequately configured; LEDs can be modulated fast and reliably via the feeding current, which also makes modulation with a specific waveform or function possible. Therefore the measurement setup can be designed in compact and efficient way by using LEDs.

With the objective to cover the wavelength range of the SR of a-Si:H solar cells we have investigated a large number of high power LEDs and determined their electrical and optical performance such as their current–voltage (I–V) curve, peak wavelength, spectral band width, etc. Data from our investigation is summarized in Table 1 containing the main operation parameters of the selected LEDs, presenting in some cases deviation from the technical data provided by the manufacturers. All the LEDs are standard commercial available models and therefore are easily exchangeable in the experimental set-up.

To supply the LEDs sine-wave generators are implemented, producing an individually optimized wave for every LED (frequency, DC bias and AC amplitude) according to the corresponding I–V curve of each LED. The light of sixteen different LEDs is superposed sweeping at frequencies between 100 Hz and 200 Hz (avoiding multiples of frequencies for the LEDs and for the 50 Hz frequency of the electricity grid) generating sinusoidal current in the solar cell. The selection of the frequency applied to each LED is important to reach a proper equipment operation, the overlap of the harmonics with the main current peaks must be avoided.

The schematic diagram of the operation of the whole system is shown in Fig. 1. The VFSR measurement system is based on an electronically controlled group of LEDs that work simultaneously as light generation source and are focused on the solar cell in a small area and on the reference photodiode. We use a fast and sensitive current metre to directly measure the generated current in both devices. The sampled time dependent current curve of the solar cell under investigation ($I_{cell}(t)$) and the reference photodiode ($I_{ref}(t)$) are analyzed through a FFT to determine the photocurrent generated by each LED ($I_{cell}(\lambda)$ and $I_{ref}(\lambda)$). We have implemented the FFT with the software platform LabView. To calculate the EQE(λ) and the I_{sc} we applied Eqs. (1)–(3) described in the previous section.

4. Results and discussion

To minimize the measurement error in our equipment we need to determine very well the peak wavelength and to select LEDs with narrow band width. Fig. 2 shows the spectra of two LEDs measured under standard operation conditions (25 °C) presenting a large difference in the band width and small differences in the peak wavelengths. We have discarded LEDs with full width at half maximum (FWHM) greater than 40 nm, in addition it is important to know the exact peak wavelength, specially for LEDs illuminating in the wavelength range at the flanges of the SR curve, to prevent large errors.

Fig. 3 presents the individual spectra for the 16 selected LEDs for the VFSR measurement system. The spectral irradiance values result from an operating point of the LEDs near to the recommended working point of the provider. Fig. 4 shows the I–V curves of some representative LEDs. The range of operation is indicated as well as their experimental DC operating point. As we can see, near

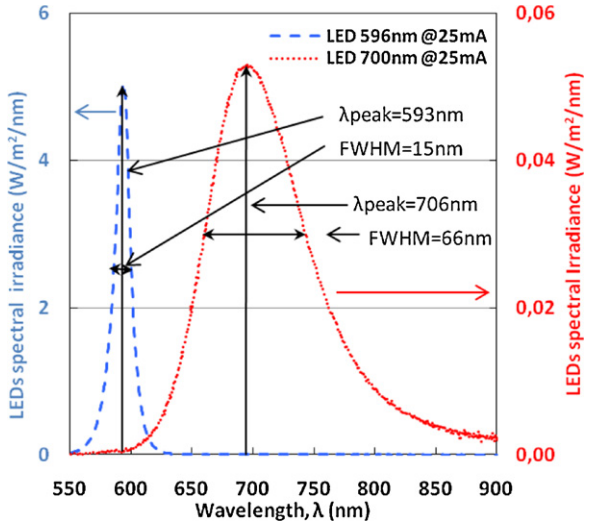

Fig. 2. Peak wavelength (λ_{peak}) and FWHM for a LED with narrow band width (22 nm, blue dashed curve) and for a LED with wide band width (66 nm, red dotted curve). (For interpretation of the references to colour in this figure legend, the reader is referred to the web version of the article.)

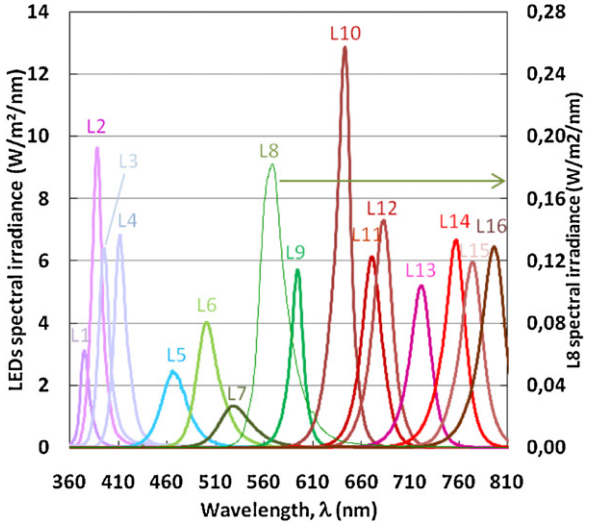

Fig. 3. Experimental spectral irradiance of the 16 selected LEDs.

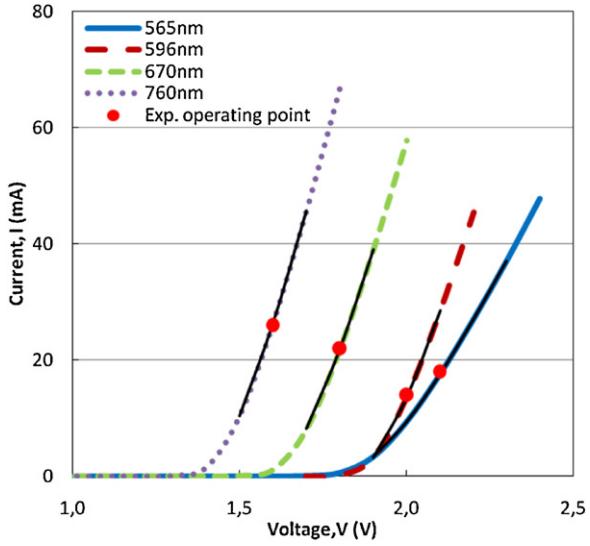

Fig. 4. Experimental *I–V* curve and DC bias point for 4 representative LEDs. The black lines indicate the AC amplitude.

the recommended working point the current–voltage relation is linear resulting in very small harmonics. The optimization of the illumination intensity of the different LEDs is still ongoing. To get similar current response on the solar cell for every wavelength we are studying the best AC amplitude and DC bias point (working point). The search for LEDs covering some gaps in the interesting wavelength range, e.g. in the near UV range, is also ongoing.

Fig. 5 shows the sampled time dependent current density curve of a 1 cm^2 solar cell fabricated with the process implemented for the production of the T-Solar modules. We measure the solar cell current for a few seconds which is sufficient for the FFT analysis since the repetition period in the time domain is about 250 ms for the applied frequency window and the frequency step width (4 Hz) in this example.

Fig. 6 presents the current density distribution in the frequency domain resulting from the current shown in Fig. 5. In the example the signal to noise ratio is about 2–4 orders of magnitude which is sufficient to determine the SR of an individual solar cell. However signal to noise ratio is objective of further improvements by optimizing the individual LED operating conditions. We use the peak

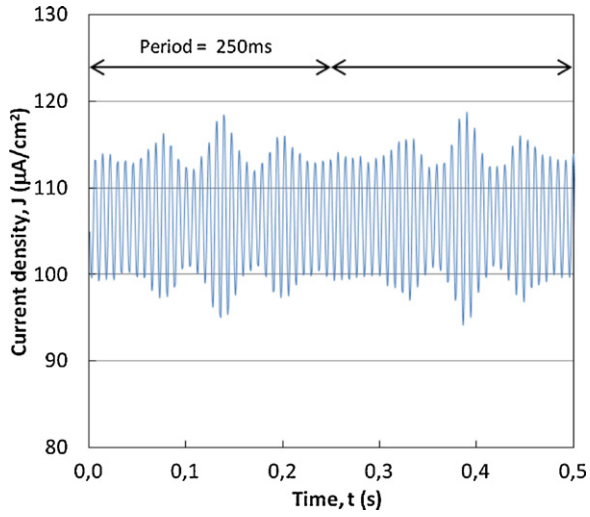

Fig. 5. Time dependent current density curve presents repetition period of 250 ms due to the selected frequencies with highest common divisor of 4.

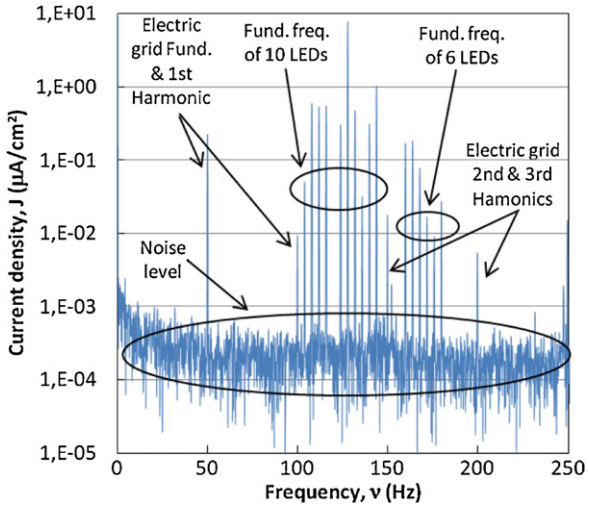

Fig. 6. Current density curve in the frequency domain as resulting from FFT analysis.

current of the fundamental excitation frequency of each LED for calibration and measurement analysis. In the figure, apart from the peaks corresponding to the LEDs, peaks resulting from the noise produced by the electricity grid are indicated.

In Fig. 7 we present the comparison of the EQE measured with our traditional equipment (continuous blue curve) and the one measured with the new VFSR equipment (red dots).

The data of the solar cell shown in Fig. 7 is measured with a solar structure of a recent T-Solar a-Si:H single junction solar module generation in the stabilized (light-soaked) state. The production process is based on a-Si:H p–i–n structure deposition on float glass with a SnO_2 transparent conductive oxide (TCO) layer. The back contact of the device consists of an ZnO TCO layer and metal coatings which act as reflectors for the light not absorbed in the first path through the pin structure [12]. Specifically the here studied cells are done in the T-Solar production line through a special laser scribe that allow to get samples of 10 cm × 10 cm

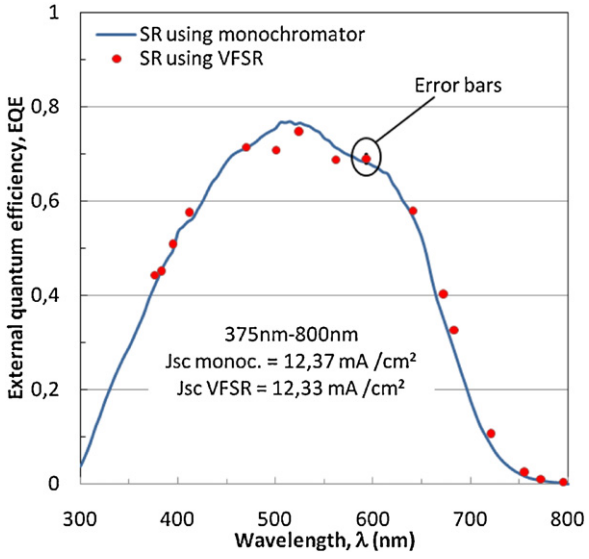

Fig. 7. The blue curve presents the EQE measured in a conventional spectral response equipment with monochromator. Red dots (the point at 593 nm has an error bar indicating its standard deviation) represent the average of ten EQE measurements with the VFSR measurement system. The difference between the J_{sc} determined with the traditional equipment and the VFSR is 0.26%. (For interpretation of the references to colour in this figure legend, the reader is referred to the web version of the article.)

with eight 1 cm^2 and two 4 cm^2 solar cells. They have an stabilized efficiency (after 300 kWh/m^2 light-soaking) of about 8.0%.

The measurement points represent the average data of ten repetitive measurements at each wavelength, for the point at 593 nm (the one with higher standard deviation) an error bar (standard deviation) is indicated. We have found that the standard deviation in repetitive measurements is less than 2% for every wavelength. For most of the points the deviation from the traditional method is small, a larger deviation is found for the LED number L6 (501 nm) and L8 (562 nm). The reason for the larger deviation at L8 most probably is due to the small intensity of the LED illumination at that wavelength which is under investigation, also the larger deviation at L6 is under investigation where we no reason have identified so far.

As shown in Fig. 7 in the insert, the short circuit current calculated in the wavelength range from 375 nm to 800 nm is very similar for both methods with a deviation of less than 1%, and comparable to values found by other researchers [1,2], making the equipment suitable for the further implementation in a mapping equipment or an in-line measurement equipment.

However, we will further optimize the LED operation to refine the VFSR. In the near UV wavelength range are still missing some measurement points due to lack of adequate LEDs. However, this is no drawback for the implementation in e.g. an mapping equipment or an in-line equipment since due to the low intensity of the AM1.5G spectrum in the range from 300 nm to 370 nm, e.g. the error in the calculation of the short circuit current is small, and the available data in the range $\lambda > 375$ nm permits to conclude on generation/recombination processes at the front contact at least in qualifying manner. In the IR wavelength range we have already implemented a high density of measurement points planning the extension of the equipment to about 1000 nm to measure amorphous silicon/microcrystalline silicon (a-Si/μc-Si) tandem solar cells.

5. Conclusions

We have developed an equipment capable of measuring the SR of a-Si:H solar cells in a few seconds. For a precise measurement of the SR a careful characterization of the implemented LEDs is necessary. Further optimization of the LED operation conditions will improve the precision of the measurement which is already better than 1% in the determination of J_{sc}. Also, the repeatability of the measurements is sufficient to perform mapping experiments on modules which is under investigation and will be reported elsewhere. Further improvement of the equipment is possible in the short wavelengths range and up-grading of the equipment to about 1000 nm for the measurement of tandem structures is in progress.

Acknowledgements

The authors like to thank O. Sampedro, E. Grande, A. Martin, F. Morel and J. Perez for their support in the development of the VFSR equipment. J.A. Rodriguez acknowledges the funding of theSpanish Ministry of Economics and Competitiveness in the frame of the program "Torres Quevedo" (Contract n° PTQ-10-03524). This work was supported by the FP7 European Project HELATHIS (Grant Agreement n°. 241378) and the regional government of Galicia (project IN841D-2010/14).

References

[1] D.L. Young, S. Pinegar, P. Stradins, B. Egaas, Proc. 33rd IEEE Photovoltaic Specialist Conference, San Diego, CA, May 11–16, 2008, NREL/CP-520-42509.
[2] W. Reetz, D. Erdweg, W. Hilgers, P. Kaienburg, A. Gerber, B. Pieters, U. Rau, Proc. 26th EU PVSEC, Hamburg, Germany, September 5–9, 2011.
[3] B.H. Hamadani, J. Roller, B. Dougherty, H.W. Yoon, Applied Optics 51 (19) (2012) 4469–4476.
[4] G. Zaid, S. Park, D.-H. Lee, S.-N. Park, Applied Optics 49 (35) (2010) 6772–6783.
[5] S. Kohraku, K. Kurokawa, Proc. 3rd World Conference on Photovoltaic Energy Conversion, Osaka, May 11–18, 2003.
[6] R.E.I. Schropp, M. Zeman, Amorphous and Microcrystalline Silicon Solar Cells: Modelling, Materials and Device Technology, Kluwer Academic Publishers, Norwell, MA, 1998, pp. 188–198.
[7] P.A. Basore, Proc. 23rd IEEE Photovoltaic Specialists Conference, Louisville, KY, May, 1993, pp. 147–152.
[8] J. Sinkkonen, A. Hovinen, T. Siirtola, E. Tuominen, M. Acerbis, Proc. 25th IEEE Photovoltaic Specialists Conference, Washington, DC, May, 1996, pp. 561–564.
[9] S. Winter, Proc. 10th NEWRAD, 2008.
[10] IEC 60904-8:1998, Photovoltaic devices-Part 8: measurement of the spectral response of a photovoltaic (PV) device.
[11] J. Metzdorf, Applied Optics (1987) 1701–1708.
[12] W. Beyer, J. Hüpkes, H. Stiebig, Thin Solid Films 516 (2007) 147–154.